NASA TECHNICAL MEMORANDUM

NASA TM X-68165

NASA TM X-68165

PERFORMANCE OF A 12-COIL SUPERCONDUCTING "BUMPY TORUS" MAGNET FACILITY

by J. Reece Roth, A. David Holmes,
Thomas A. Keller and Walter M. Krawczonek
Lewis Research Center
Cleveland, Ohio

TECHNICAL PAPER prepared for presentation at
Texas Symposium on the Technology of Controlled Thermonuclear Fusion Experiments and the Engineering Aspects of Fusion Reactors
Austin, Texas, November 20-22, 1972

PERFORMANCE OF A 12-COIL SUPERCONDUCTING "BUMPY TORUS" MAGNET FACILITY

by J. Reece Roth, A. David Holmes,
Thomas A. Keller and Walter M. Krawczonek

NASA Lewis Research Center
Cleveland, Ohio 44135

E-7225

ABSTRACT

The NASA-Lewis "bumpy torus" facility consists of 12 superconducting coils, each 19 cm i.d. and capable of 3.0 tesla on their axes. The coils are equally spaced around a toroidal array with a major diameter of 1.52 m, and are mounted with the major axis of the torus vertical in a single vacuum tank 2.6 m in diameter.

Final shakedown tests of the facility mapped out its magnetic, cryogenic, vacuum, mechanical, and electrical performance. The facility is now ready for use as a plasma physics research facility. A maximum magnetic field on the magnetic axis of 3.23 teslas has been held for a period of more than sixty minutes without a coil normalcy. The design field was 3.00 teslas. The steady-state liquid helium boil-off rate was 87 liters per hour of liquid helium without the coils charged. The coil array was stable when subjected to an impulsive loading, even with the magnets fully charged. When the coils were charged to a maximum magnetic field of 3.35 teslas, the system was driven normal without damage.

INTRODUCTION

A modest research program is underway at the NASA Lewis Research Center to investigate the problem of ion heating, high temperature plasma physics, and of thermonuclear power production which are unique to space applications (ref. 1).

The bumpy torus concept shown in figure 1 was proposed in reference 2 as one basis for further research in these areas. This concept consists of 12 superconducting magnetic field coils arranged end-to-end in a toroidal array. The ions which, in a mirror geometry, would be lost to the vacuum tank wall, are constrained by the magnetic field lines to circulate around the major circumference of the torus. It is anticipated that the reduction of end losses associated with a magnetic mirror geometry will permit substantially higher particle densities and confinement times to be achieved.

The number of field coils, the major and minor diameters of the toroidal array, and the design magnetic field strength were the result of an economic optimization described in reference 3. The major characteristics of the bumpy torus geometry are listed in Table 1, and result from maximizing the volume of confined plasma per dollar, subject to the constraint of adiabatic confinement of 10 keV deuterium ions.

The scope of this paper is restricted to data on the mechanical, electrical, cryogenic, and magnetic design and performance of the magnet facility discussed. The phenomena observed, and results

obtained in plasma-physical investigations in this facility are not covered. A retrospective summary of the performance of the superconducting "pilot rig" facility which preceded the bumpy torus, the design philosophy of the bumpy torus, and a detailed description of the superconducting magnets have been given in other publications (ref. 4 and 5).

FACILITY DESCRIPTION

A photograph of the facility is shown in figure 2, which shows the assembled coil array inside the vacuum tank before installation of the vacuum tank lid. The 12 superconducting coils with their liquid nitrogen cooled covers are visible. Four spacer bars have been installed between each pair of coils and the spacer bars are covered in turn by a heat shield maintained at liquid nitrogen temperature by conduction from the coil covers on either side. The very good access to the experimental volume by the pumping system is evident, with the diffusion pump opening occupying the center portion of the toroidal array.

Above the coils are the liquid nitrogen temperature shields which surround the liquid helium reservoir tanks. There are three such reservoirs, each with a capacity of 100 liters of liquid helium. The entire coil assembly and the upper liquid helium manifold are suspended from two force-bearing yokes at either end of each of the three reservoir tanks. The weight of the magnet sub-assembly is ultimately supported by nine brackets, three at the bottom of each liquid helium reservoir.

The venting helium gas rises through the upper connection to the coil canisters to the upper liquid helium vent manifold, and through a standpipe to the top of the three liquid helium reservoirs. The vented gas travels along the top of the reservoirs and out gaseous helium vent lines located at two stations in the vacuum tank. One of the gaseous helium vent lines also contains the coil power leads and the coil sensor leads, which are cooled by the venting helium gas.

On figure 3 is shown a photograph of the exterior of the vacuum tank. The catwalk which surrounds the upper portion of the tank is used to gain access to the upper airlocks through which the experimental apparatus is inserted into the system. Around the midplane of the tank, approximately at normal eye level, are 12, 25.4 cm diameter ports. Ten of the 12 circumferential viewports look directly in on the midplane of the plasma, half-way between adjacent coils. Two of the viewports are canted at an angle, which permits instruments and probes to be inserted approximately tangentially to the magnetic field lines in the confinement volume. There are also 12, 15.2 cm diameter ports at the bottom of the tank, which are aligned with the midplanes half-way between adjacent coils. Six of these 12 ports are required for liquid nitrogen service lines and other service equipment. Six of the 12 positions are available for the insertion of probes through the bottom of the tank.

FACILITY PERFORMANCE

Superconducting Coil Performance

A detailed design of the 12 individual coils was undertaken when the overall characteristics of the bumpy torus were determined by the economic optimization described in reference 3. The 12 coils are virtually identical in their geometry and number of ampere turns. Round and square conductor was used as indicated in Table II. This coil design was arrived at with the assistance of members of the Magnetics and Cryophysics Branch of the Physical Science Division at the Lewis Research Center. The characteristics and performance of these coils have been described elsewhere (ref. 4,5).

Each of the 12 coils comprising this facility was individually tested and met or exceeded its designed current before being incorporated in the facility. The performance of these coils during their individual tests is summarized on Table II. The result of testing the superconducting coil performance in the complete array is summarized in references 4 and 5. It was found that the entire array could be held at a maximum magnetic field on the magnetic axis of 3.23 teslas for at least one hour, which compared with the designed magnetic field of 3.00 teslas. It was found that the facility went normal at a magnetic field of 3.35 teslas. In figure 4 is shown a survey of the magnetic field across the equatorial plane of the torus midway between two adjacent coils, normalized to a relative magnetic field of 0.403 on the magnetic axis. There is agreement within 3 percent with the relative magnetic field taken from numerical computations for the

complete coil array.

Figure 5 shows a plan view of the magnetic field lines in the equatorial plane of the torus. The magnetic field lines neck down in the region of maximum field strength under the coils, and bow out in the regions between adjacent coils.

Mechanical Performance

With equal currents in all coils, the magnetic forces acting on a coil will be very nearly in equilibrium due to the equal and opposite forces on adjacent coils. Because the 12 coils are tilted with respect to each other by 30^{o} in this toroidal array, the resultant will be a small compressive force tending to draw the 12 coils to a smaller major radius. The worst possible disposition of mechanical forces that can arise in this facility occurs when only a few adjacent coils have superconducting currents flowing in them. In order to test the mechanical and cryogenic design of the facility before the entire assembly was put together, a coil pair test was performed in another vacuum tank with a canted pair of coils.

In figure 6 is shown a photograph of the coil pair test rig. The major radius of curvature of this test rig was identical to that on the completed facility. Two of the coils and liquid nitrogen can covers used in the final facility were used in this test. The spacer bars on the outside of the two coils were used to brace the coil pair assembly against the walls of the 1.5 meter diameter vacuum vessel in which the test was performed. The coils were connected to an upper

and lower liquid helium manifold. The reservoir was of a substantially different design from those used in the facility.

The two coils in the configuration shown in figure 6 have the maximum possible compressive forces acting between them and hence provide a worst possible test case of the spacer bars and the other structural elements of the coil assembly. These two coils were energized up to a maximum magnetic field of 3.50 teslas and were able to hold this magnetic field for more than 5 minutes without mechanical deformation or failure.

The coil pair assembly shown in figure 6 contained 13 A&N fittings at liquid helium temperature. In the coil pair test there were no leaks from the liquid helium system into the vacuum tank during the cool-down process, during the coil charge-up, or during the coil normalcy when there was a backpressure in the system. Possible leaks of helium into the vacuum system were monitored by a leak detector on its most sensitive scale. This indicated no helium leak whatever into the vacuum tank during the test.

An important feature of the mechanical performance of the 12 coil array, which could not be adequately simulated in the coil pair test, was the stability of the ring of 12 coils with compressive magnetic forces acting between them. It was considered possible that the array of 12 coils, in spite of the spacer bars, and the rigidity of the upper liquid helium manifold to which the assembly is attached, might be subject to a form of torsional instability which is illustrated by an O-ring which can be folded from a single hoop into a three-turn hoop.

To monitor the stability of the coil array, a system was employed very similar to that used to monitor the flutter stability of airplane wings without destroying the aircraft. This system consisted of strain gauges, which were capable of operating at liquid helium temperatures, on one of the outer spacer bars. The pivoted hammer shown in figure 2 delivered a fixed impulse to a spacer bar, which excited the elliptical modes of oscillation of the entire coil array.

As the coils were charged up for the first time, the magnet current was taken up in increments of 50 amps to the limit of 650 amperes. At each 50 amp increment, an impulse was given to the coil array. The elliptical mode vibrations induced in the coil array were observed with an oscilloscope hooked up to the strain gauge.

If the system is stable, the oscillations induced by the impulsive blow will die away, yielding an exponentially decreasing oscillation waveform. If the system is unstable, the oscillations will grow until the magnet assembly collapses. At each 50 ampere increment, the effective decay constant of the impulsively induced oscillations was measured. On figure 7 is shown oscillographs of the response of the magnet system to an impulsive excitation for magnet currents ranging from 350 to 625 amperes. Each one of the oscillographs similar to figure 7 had a characteristic e-folding decay constant, α , given by the formula

$$A = A_o e^{-\alpha t}$$

So long as α is positive, this implies an exponentially decaying

waveform similar to that in figure 7, and the magnet facility is stable at that magnet current. If the value of α decreases and extrapolates to zero somewhere in the designed range of operating currents, the magnet facility is unstable.

As one can see in figure 7, however, α is virtually constant, and the system is stable over the entire range of operating currents.

Performance of Cryogenic System

On figure 8 is an isometric view of a liquid nitrogen can cover showing the inner bore cooling. The liquid nitrogen is forced to flow through a system of zigzagged axial passages. This design was intended to minimize the amount of radial space taken by the cooling passages, while at the same time permitting the removal of a substantial loading or radiant energy from the plasma. The liquid nitrogen can cover was made of copper, and chrome plated to minimize the amount of absorbed gases and dirt acquired during the fabrication and assembly process. The remainder of the liquid nitrogen heat shield is cooled by .95 cm diameter copper tubing, which is welded to the sheet metal base.

The liquid nitrogen can covers on each coil contain eight A&N fittings. These were necessary to break the connections of the coil covers to the manifolds. Each of the four lines connecting the two liquid nitorgen circuits to their manifolds contained a stainless steel bellows to permit final fitting of the coil in position. It was found that A&N fittings could be used for liquid nitrogen service in a vacuum system, if copper tubing is mated to male stainless steel fittings.

In the liquid nitrogen system, it was also found that reliable joints required that the mating surfaces be covered with teflon tape before the surfaces were mated. A higher than normal torque was desirable to reliably make a tight connection.

In the liquid nitrogen tubulation there were approximately 96 A&N fittings in the liquid nitrogen lines. There were approximately 420 silver soldered connections in the entirety of the liquid nitrogen flow system. The liquid nitrogen shields surrounding the 12 coils, and the liquid nitrogen shield surrounding the liquid helium reservoirs above them, present approximately 18 square meters of liquid nitrogen temperature surfaces to the vacuum tank and provide a substantial cryopumping of impurity gases such as CO_2, water vapor, and any pump oil that might otherwise be present to contaminate the experiment. It was intended that the liquid nitrogen flow through each of the 12 coil shields be adequate to remove 2 kW of power.

An innovation in this facility is the use of 1" A&N fittings in the liquid helium system. Until the canted coil pair test for this facility, it was not clear whether standard A&N fittings could be used at liquid helium temperatures in a vacuum environment without leaks appearing after multiple thermal cycles. Altogether this magnet facility contains 36 A&N fittings at liquid helium temperatures, and it also contains 24 stainless steel bellows between the coils and the upper and lower liquid helium manifolds. Special precautions were taken to prevent leaks from developing when A&N fittings are used at liquid helium temperatures and in a vacuum environment. These

precautions included using teflon tape between mating surfaces, and torquing the fittings to at least 100 ft-lbs (135 newton-meters) in order to assure a leak-tight connection.

The liquid helium system and the coils were cooled from room temperature to temperatures approaching that of liquid nitrogen by evacuating the large vacuum tank, and allowing liquid nitrogen to flow through the liquid nitrogen heat shields. The temperature of the liquid nitrogen system was monitored with thermocouples at several locations. The results of a cool-down to liquid nitrogen temperature are shown in figure 9. Illustrated are two curves, including one of the 12 LN_2 coil shields, and the midpoint of a long spacer bar cover.

When the system was approximately at -40°C, the liquid helium system was cooled to temperatures approaching that of liquid helium by passing liquid helium through the system from the mobile dewar outside the building. The amount of liquid helium required to cool the system from -40°C to liquid helium temperatures was approximately 2300 liters.

The apparatus used to measure the liquid helium boil-off consisted of a bypass in the liquid helium vent line in which the venting helium gas passed through a heater, and a meter which measured the integrated gas flow through the system. The steady-state liquid helium boil-off rate was measured after loading, with the reservoirs initially filled, when the system seemed to be equilibrated, both with and without the magnets being charged up. The boil-off rate without the magnets

charged was 87 liters per hour of liquid helium. The boil-off rate, when the magnets were charged up to their rated field of 3.0 teslas, was 100 liters per hour. At B_{max} = 2.4 teslas, the boil-off rate was 95 liters per hour. The boil-off performance of the system was measured during magnet charge-up. These magnet chargings started with no current, and ended at the rated field strength of 3.0 teslas. The additional boil-off is approximately 14 liters for the charging process, at a ramp rate of 90 amps/minute.

The backpressure in the liquid helium system was measured during a coil normalcy which took place at B_{max} = 3.30 tesla. It was found that the pressure at the top of the liquid helium reservoirs was 17.2 lbs/sq in. absolute (1.18×10^5 newtons/m^2). During a coil normalcy at B_{max} = 3.0 teslas, approximately 140 liters of liquid helium were boiled off. A normalcy at B_{max} = 3.30 teslas boiled off 210 liters of liquid helium. When one coil in the system went normal first, this triggered from one to six other coils to go normal. The facility has undergone 22 normalcies at the present writing. No apparent damage occurred to the coils as a result of the coil normalcies.

The effectiveness of the liquid nitrogen can covers in carrying away radiant energy was measured with a radiant heat loading assembly. This assembly consisted of 8 quartz lamps which were energized with a Variac and could irradiate the inner bore of one of the 12 superconducting coils with a known amount of radiant energy. It was desired to see at what point vapor lock would occur in the liquid nitrogen cooling passages on the inner bore of this coil, and also to see how much of

the radiant energy eventually appeared in the liquid helium canister. No difference in the boil-off rate of liquid helium was noted, even with 3 kilowatts loading on the inner bore of the liquid nitrogen heat shield. On figure 10 is shown the temperature of the midpoint of the inner bore of the shield, as a function of time and of the power into the heat load. The fluctuations in temperature are probably due to vapor lock or film boiling.

Vacuum System Performance

Performance of the A&N fittings was measured by monitoring the background partial pressure of helium, oxygen, and nitrogen in the vacuum tank at room temperature, as the liquid helium system was cooled down, as it was filled with liquid helium, as the magnets were charged, and finally as the magnets went normal. The performance achieved in the coil pair test was repeated in the test of the facility as a whole. At the present writing the system has undergone 3 thermal cycles from room temperature to liquid helium temperatures, 22 coil normalcies, and 40 cycles of charging and discharging the coil assembly without any serious leakage problem from the A&N fittings in either the liquid nitrogen or liquid helium systems. Approximately four month's time and six man-months of effort were required to eliminate all significant leaks from the liquid nitrogen and liquid helium systems into the vacuum tank in which they were enclosed. In the liquid nitrogen system, nearly all leaks were associated with silver solder joints, or copper welds in the liquid nitrogen can covers. In the liquid helium

system, the leaks were associated with stainless steel welds, or with stainless steel bellows which were pitted by corrosion associated with silver solder flux. The A&N fittings in both systems presented no leakage problems whatever.

With all components of the system at room temperature (except the liquid nitrogen cold trap above the diffusion pump), the leakage from the liquid nitrogen system into the vacuum tank contributed a partial pressure of less than 5×10^{-10} torr to the tank background pressure. Leakage from the liquid helium system into the tank contributed less than 3.5×10^{-9} torr to the background pressure. At liquid nitrogen temperature, the leakage from the liquid helium system into the vacuum tank contributed a partial pressure of less than 5×10^{-10} torr to the tank background. With liquid helium in the liquid helium system, the leakage of helium from it contributed a partial pressure of less than 2×10^{-8} torr.

The vacuum tank is evacuated by a 300 CFM (141 liter/sec) mechanical forepump which is connected to a 32" (81 cm) oil diffusion pump with a rated pumping speed of 32,000 liters per second. The diffusion pump was filled with silicone 705 oil. Between the diffusion pump and the vacuum tank was a liquid nitrogen cold baffle to prevent back-streaming of the diffusion pump oil into the vacuum tank. Between the vacuum tank volume and the liquid nitrogen baffle was a pumping speed controller, which permits independent variation of the background pressure and pumping speed of the pumping system.

A photograph of the pumping speed controller is shown in figure 11. Figure 11a shows the pumping speed controller with its flaps open, figure 11b shows the pumping speed controller with the flaps closed. These flaps are not intended to be vacuum tight, but merely to control the cross-sectional area of the pumping system. It is anticipated that several experimental applications will necessitate an independent control of the pumping speed and the background pressure. This may be accomplished by altering the angle of the flaps in the pumping speed controller.

The effect of the pumping speed controller can be seen in figure 12, which shows the pressure of the vacuum system as the angle of the flaps in the pumping speed controller is changed. The calibrations on the x-axis of figure 12 represent the angle of the flaps with respect to the horizontal. These measurements were made with a constant throughput of 0.68 torr-liters/sec of deuterium gas. The effect of the incremental pumping speed caused by cold cryogenic surfaces in the vacuum tank may be seen in figure 13.

The background pressure of the system with all of the coil components at room temperature and after 62 hours of pumping was 4.5×10^{-7} torr. When both the liquid nitrogen and liquid helium systems were at liquid nitrogen temperatures, the background pressure of the vacuum system after 20 hours was reduced to 3.8×10^{-7} torr. When the liquid helium system was taken to liquid helium temperatures, additional cryopumping reduced the background pressure of the system

after 6 hours to 2.2×10^{-7} torr. These measurements were made with the pumping speed controller in the open position. The partial pressure of background contaminants was monitored with a mass spectrometer and it was found that the principal contaminants were about equally divided between air and water vapor with the components in the tank at room temperature. With the magnets charged to 3.0 teslas, the background consisted of 90 percent air and 10 percent helium gas. The pumping speed curves for deuterium gas are shown in figure 13.

Performance of Instrumentation and Electrical System

In a facility of this nature, it is essential to know the liquid helium level in all components of the system which are supposed to be at liquid helium temperatures and contain superconducting wire. Knowledge of the liquid helium level is particularly important during early stages of facility testing before a body of experience is acquired to guide operating practice.

Liquid helium level sensors were installed at the bottom and top of the liquid helium cans of all 12 coils. The bottom-most sensor indicated when liquid helium was starting to accumulate in the system. The high level sensor in each of the 12 coils indicated if a vapor lock or other difficulty existed in any particular coil, and they also served to warn that the liquid helium level was dangerously low at the end of a run. In addition to these sensors, there were 8 liquid level sensors at equally spaced intervals in the three liquid helium reservoir tanks. Altogether there were liquid helium level sensors in 48

different locations throughout the system. Each one of these 48 positions had a redundant spare.

The 12 coils were hooked up in series, with only two leads connecting the coil assembly to the power supply outside the liquid helium environment. The voltage drop across each of the 12 coils was monitored by sensor leads attached to the coil. The coil power supply has a capacity of 1000 amps and 20 volts. This power supply is permanently connected to the coils, and current flows through the coils at all times when the magnets are charged. The power supply is controlled by a ramp-and-hold circuit which permits a programmed ramp rate to a pre-selected magnet current.

It was intended that the vacuum system of this facility operate unattended overnight and over weekends. For this reason a comprehensive interlock system was used to shut the system down in the event of a failure of vacuum pressure, or of building power, water, or air. In addition to provisions to assure an orderly shutdown of the system in the event of a failure of the building services, a number of interlocks and protective circuits are associated with possible modes of failure during experimental operation.

This facility contains 48 thermocouples placed in the liquid helium and liquid nitrogen portions of the system. These thermocouples are useful in monitoring the cool-down from room temperature, and the heat load deposited on the system by the plasma.

Of a total of 96 liquid helium level sensors, it was found that

five were open-circuited immediately before the system was cooled down to cryogenic temperatures for the first time. These open circuits may have resulted from mechanical shock or vibration during the assembly or welding process. After the system experienced one thermal cycle from room temperature to liquid helium temperatures, 2 additional liquid helium sensors showed an open circuit or other defects in their operation. However, because a redundant liquid helium level sensor was available at each location, all 48 of the stations indicated the liquid helium level.

The performance of the coil power supply was quite satisfactory. It ramped up to the rated field and down automatically, and produced no unanticipated behavior during the coil charging process.

REFERENCES

1. Roth, J. Reece; Rayle, W. D.; and Reinmann, J. J.: Technological Problems Anticipated in the Application of Fusion Reactors to Space Propulsion and Power Generation. NASA TM X-2106, Oct. 1970.

2. Roth, J. R.: Plasma Stability and the Bohr-van Leeuwen Theorem. NASA TN D-3880, April 1967.

3. Roth, J. R.: Optimization of Adiabatic Magnetic Mirror Fields for Controlled Fusion Research. NASA TM X-1251, July 1966.

4. Roth, J. Reece; Holmes, A. David; Keller, Thomas A.; and Krawczonek, Walter M.: A 12-Coil Superconducting "Bumpy Torus" Magnet Facility for Plasma Research, NASA TM X-68063, Presented at the Applied Superconductivity Conference, Annapolis, Maryland, May 1-3, 1972.

5. Roth, J. Reece; Holmes, A. David; Keller, Thomas A.; and Krawczonek, Walter M.: Characteristics and Performance of a 12-Coil "Bumpy Torus" Magnet Facility for Plasma Research, NASA TN D- (to be published).

TABLE I

DESIGN CHARACTERISTICS OF THE NASA-LEWIS

BUMPY TORUS MAGNETIC FACILITY

Major diameter of torus	1.52	meters
Inside diameter of spoolpiece	21.0	cm
Inside diameter of coil winding	21.8	cm
Outside diameter of coil winding	30.5	cm
Axial width of coil windings	12.0	cm
Design current for individual coil	700	amps
Maximum magnetic field on axis of a single coil at 700 amps design current	3.00	teslas
Maximum magnetic field on magnetic axis of entire toroidal array	3.00	teslas
Mirror ratio on magnetic axis	2.48:1	

TABLE II

INDIVIDUAL COIL PERFORMANCE DATA

Coil No.	Position in Toroid	Wire Type	Number of Turns on Coil	Charging Rate Range Amps/min	Maximum Holding Current Amps	Maximum Holding Magnetic Field Teslas	Figure of Merit, Gauss (10^{-4} Tesla)/amp
1	0°	Round	977	45-240	750	3.10	41.3
2	30°	Square	977	90-450	800	- *	- *
3	60°	Square	977	50-250	800	- *	- *
4	90°	Square	974	120-500	800	- *	- *
5	120°	Square	977	60-180	750	3.04	40.5
6	150°	Square	977	30-240	750	3.05	40.7
7	180°	Square	977	60-180	752	3.05	40.4
8	210°	Square	977	30-180	755	3.06	40.4
9	240°	Round	977	45-240	750	3.11	41.5
10	270°	Round	977	40-460	850	3.56	41.9
11	300°	Round	973	45-240	850	3.57	42.0
12	330°	Round	977	45-240	852	3.58	42.0
						Average	41.2

*Magnetic field measurements not available

FIGURE CAPTIONS

Figure 1 - A schematic drawing of the bumpy torus concept.

Figure 2 - Photograph of the completely assembled coil array inside the vacuum tank.

Figure 3 - A photograph of the exterior of the vacuum tank.

Figure 4 - The measured magnetic field as a function of radius in the midplane between two coils, normalized to a relative magnetic field of 0.403 on the magnetic axis.

Figure 5 - Magnetic field line distribution in the equatorial plane of the torus.

Figure 6 - A photograph of the coil pair test rig.

Figure 7 - Oscillographs of the response of the magnet system to an impulsive excitation. Horizontal scale is 10 msec per major division.

Figure 8 - An isometric view of a liquid nitrogen can cover showing the provision for cooling the inner bore of the cover.

Figure 9 - The liquid nitrogen can cover temperature as a function of time during cool-down from room temperature to liquid nitrogen temperature.

Figure 10 - Graph of temperature of center point of bore of liquid nitrogen heat shield as a function of time and heat load.

Figure 11 - Photographs looking vertically downward on the pumping speed controller.

Figure 11a - The pumping speed controller with the flaps open.

Figure 11b - The pumping speed controller with the flaps closed.

Figure 12 - Effect of pumping speed controller.

Figure 13 - Pumping speed as a function of tank pressure for deuterium gas.

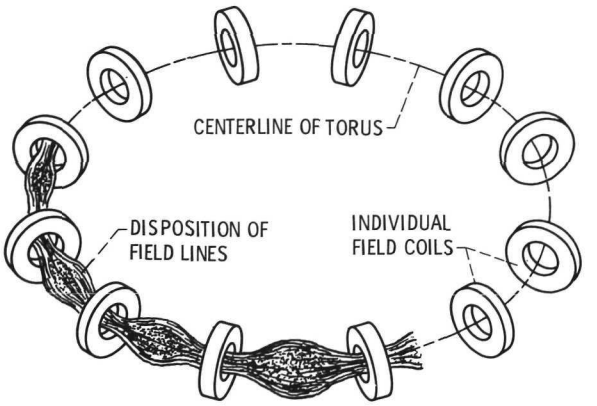

Figure 1. - A schematic drawing of the bumpy torus concept. Twelve superconducting magnets are arranged so that the plasma forms a toroidal volume.

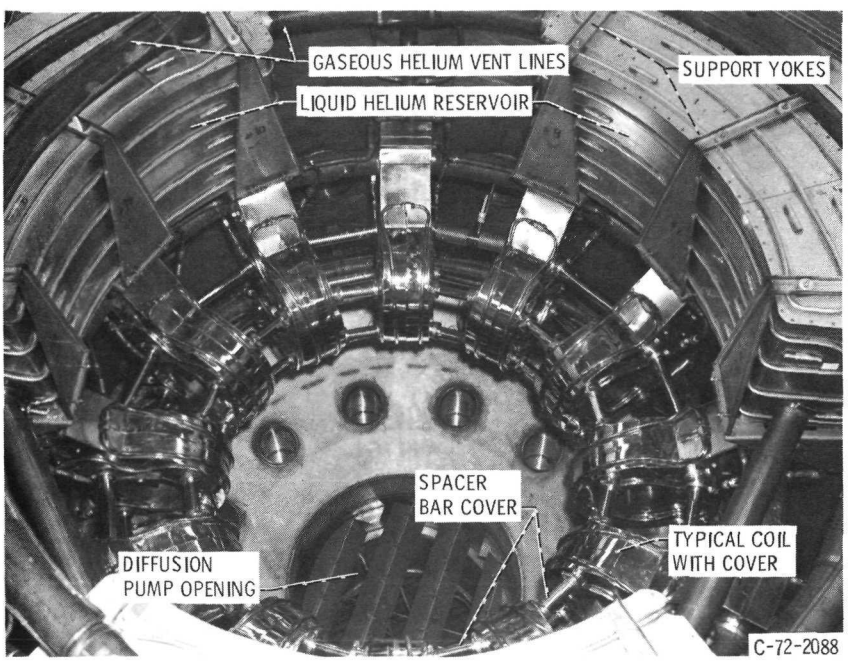

Figure 2. - Photograph of the completely assembled coil array inside the vacuum tank and before the vacuum tank lid was set in place.

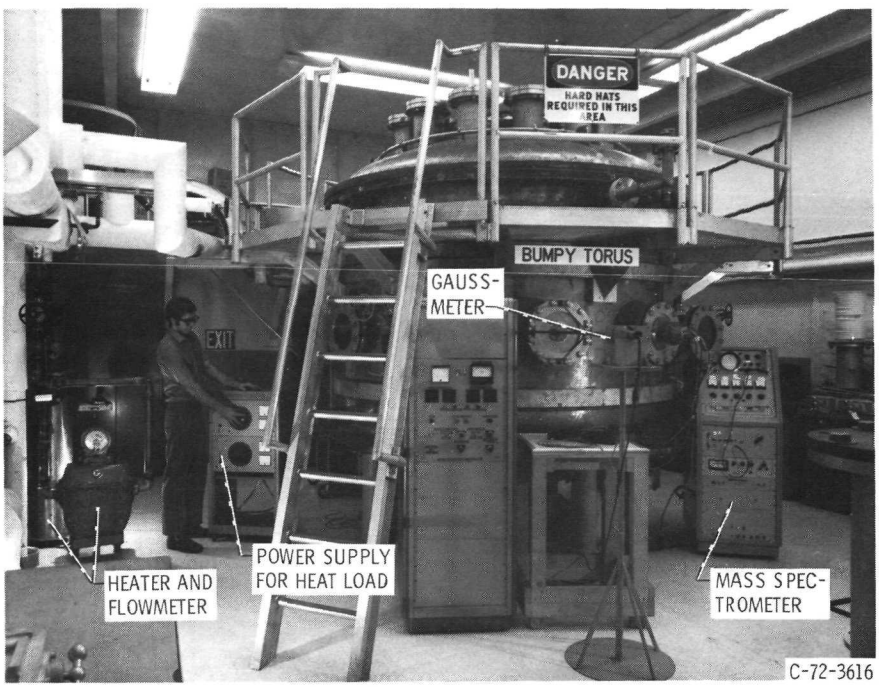

Figure 3. - A photograph of the exterior of the vacuum tank with the lid in place.

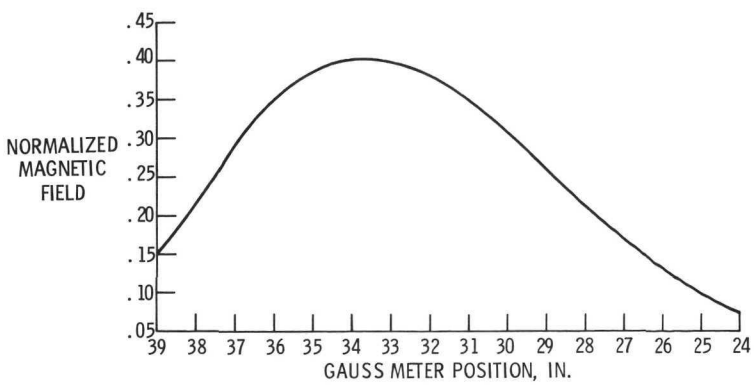

Figure 4. - The measured magnetic field as a function of radius in the midplane between two coils, normalized to a relative magnetic field of 0.403 on the magnetic axis.

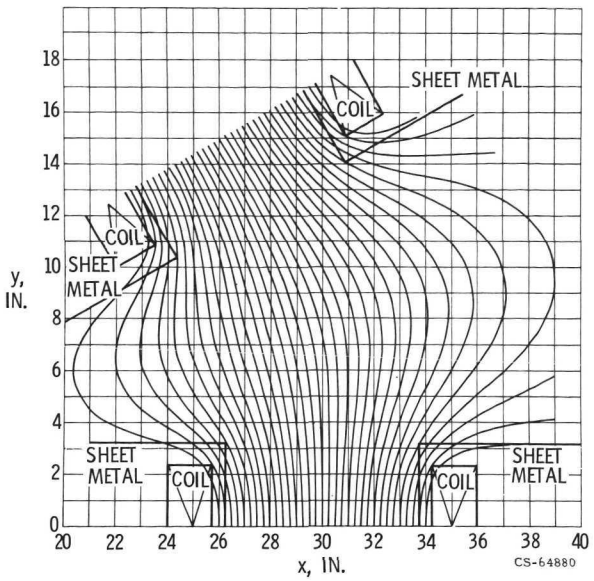

Figure 5. - Magnetic field line distribution in the equatorial plane of the torus.

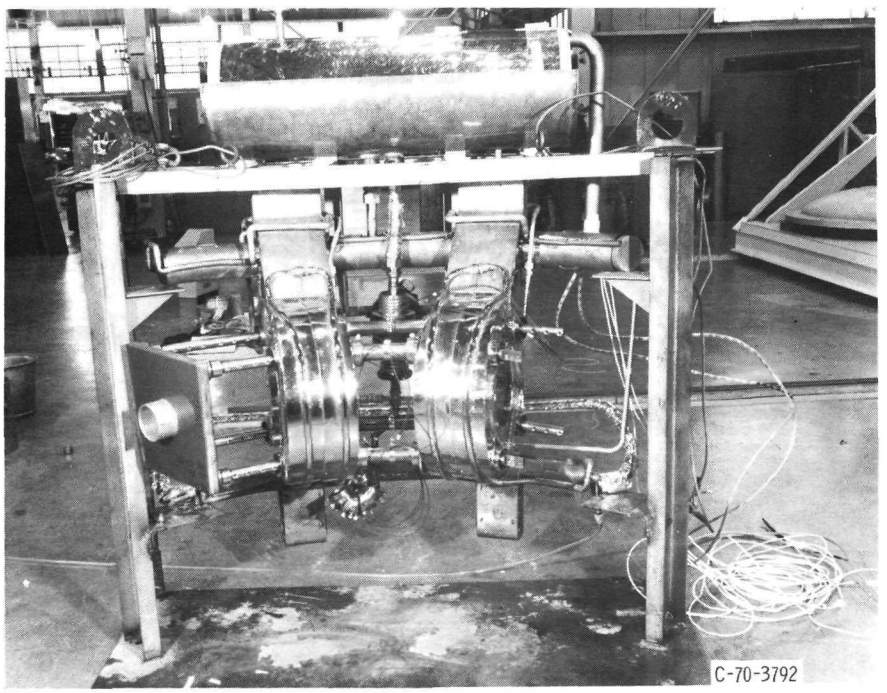

Figure 6. - A photograph of the coil pair test rig which was designed to test the mechanical and cryogenic performance of the design.

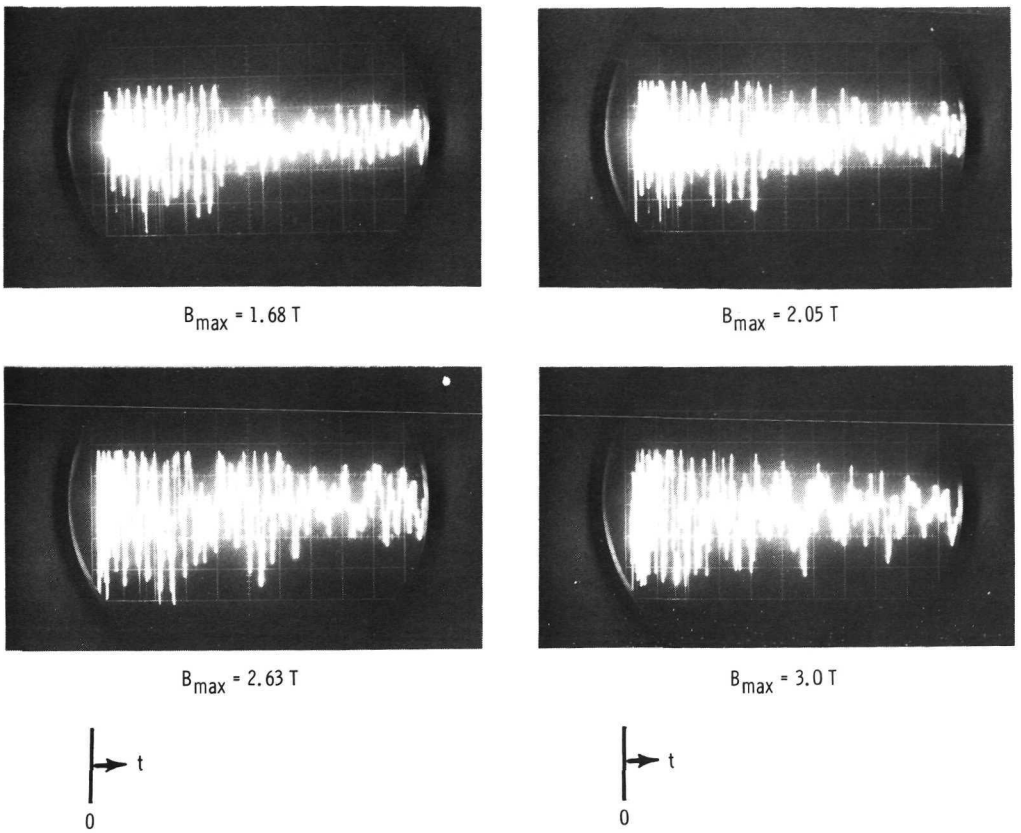

10 MS/CM

Figure 7.

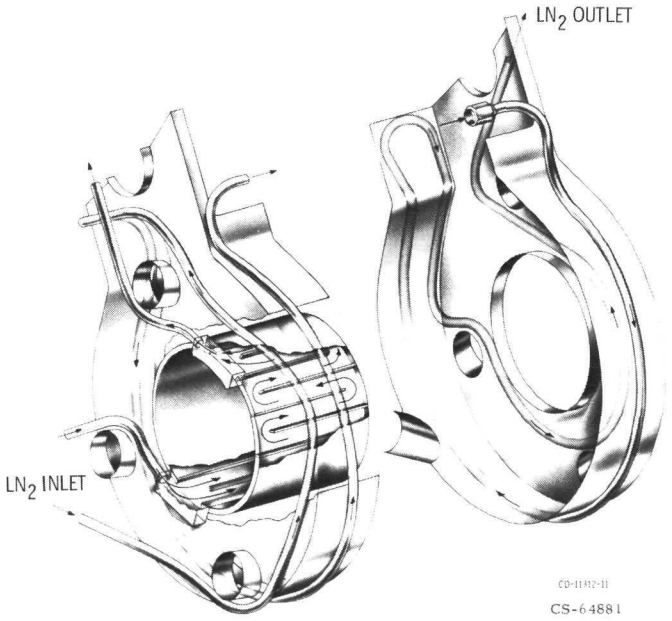

Figure 8. - An isometric view of a liquid nitrogen can cover showing the provision for cooling the inner bore of the cover.

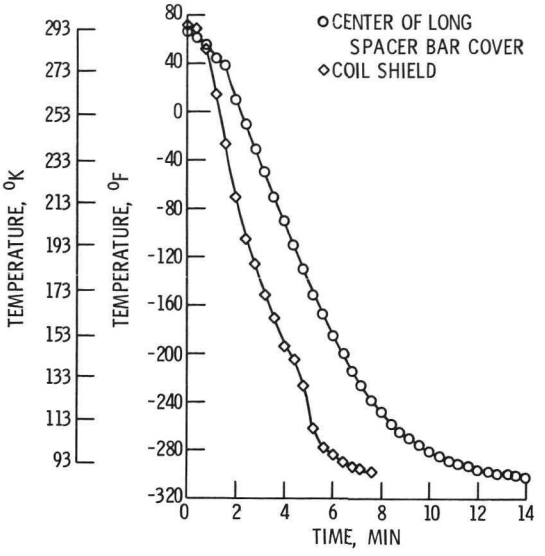

Figure 9. - The liquid nitrogen can cover temperatures as a function of time during cool-down from room temperature to liquid nitrogen temperature.

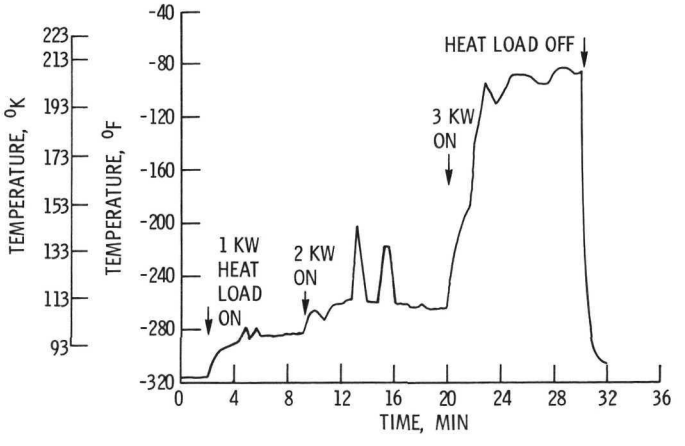

Figure 10. - Graph of temperature of center point of bore of liquid nitrogen heat shield as a function of time and heat load.

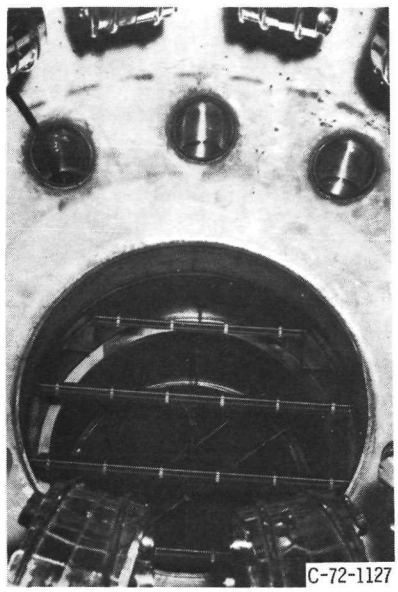

(a) FLAPS OPEN.

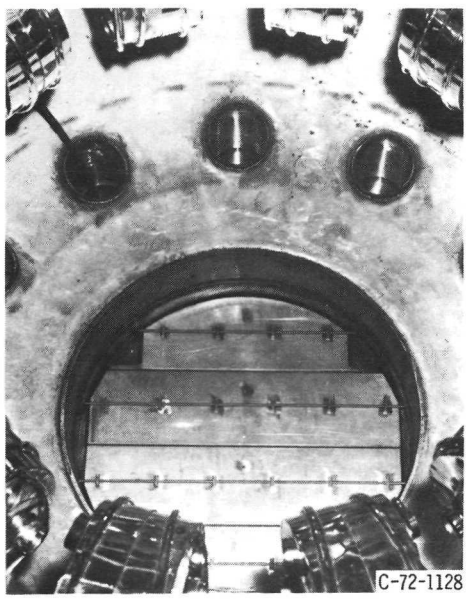

(b) FLAPS CLOSED.

Figure 11. - The pumping speed controller.

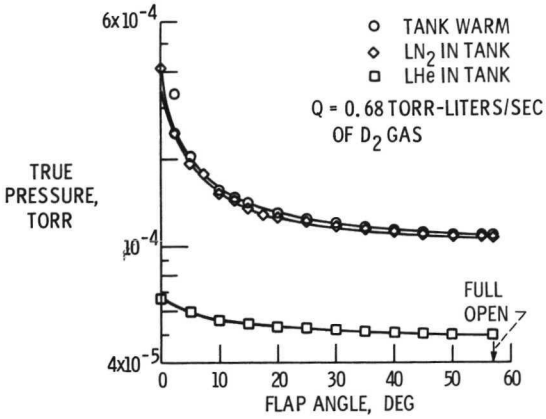

Figure 12. - Effect of pumping speed controller.

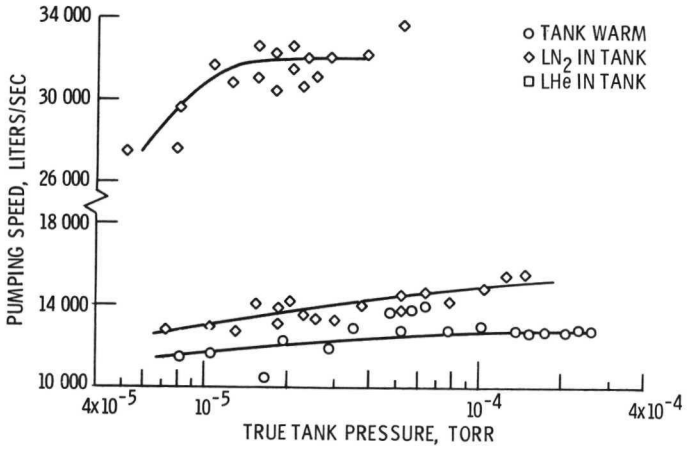

Figure 13. - Pumping speed as a function of tank pressure for deuterium gas.